



HAL
open science

Sorption–Deformation–Percolation Model for Diffusion in Nanoporous Media

Chi Zhang, Ali Shomali, Benoit Coasne, Dominique Derome, Jan Carmeliet

► **To cite this version:**

Chi Zhang, Ali Shomali, Benoit Coasne, Dominique Derome, Jan Carmeliet. Sorption–Deformation–Percolation Model for Diffusion in Nanoporous Media. *ACS Nano*, 2023, 17 (5), pp.4507-4514. 10.1021/acsnano.2c10384 . hal-04236127

HAL Id: hal-04236127

<https://cnrs.hal.science/hal-04236127v1>

Submitted on 10 Oct 2023

HAL is a multi-disciplinary open access archive for the deposit and dissemination of scientific research documents, whether they are published or not. The documents may come from teaching and research institutions in France or abroad, or from public or private research centers.

L'archive ouverte pluridisciplinaire **HAL**, est destinée au dépôt et à la diffusion de documents scientifiques de niveau recherche, publiés ou non, émanant des établissements d'enseignement et de recherche français ou étrangers, des laboratoires publics ou privés.

1 Adsorption/percolation model for water diffusion in 2 deformable nanoporous polymers

3 *Chi Zhang^{†*}, Ali Shomali, Benoit Coasne[‡], Dominique Derome[§], Jan Carmeliet[†]*

4 [†] Chair of Building Physics, Department of Mechanical and Process Engineering, ETH
5 Zurich, Raemistrasse 101, 8092 Zurich, Switzerland.

6 [‡] Université Grenoble Alpes, CNRS, LIPhy, 38000 Grenoble, France

7 [§] Department of Civil and Building Engineering, Université de Sherbrooke, Sherbrooke J1K
8 2R1, Québec, Canada

9 * Corresponding Email: outlook.zhangchi@gmail.com

10

11 **Abstract**

12 Molecules diffusing in porous media exhibit complex dynamics when their size approaches the
13 pore length scale and strong guest-host forces are at play – as is the case for water diffusion in
14 a dense, adsorbing and deformable polymer. The intricate nature of diffusion impedes the
15 complete understanding of the mechanisms, despite the fundamental relevance to numerous
16 important applications. Here, molecular dynamics simulations are used to formulate a
17 theoretical framework that sheds light on the intermittent dynamics of confined water molecules
18 and its link with the material structure as well as its physical behavior (sorption and
19 deformation). By analyzing water trajectories, we determine the moving and waiting times as
20 well as the switching frequency to predict the microscopic self-diffusion coefficient. The
21 apparent tortuosity, defined as the ratio of the bulk to the confined self-diffusion coefficients,
22 is found to depend quantitatively on a limited set of material parameters: heat of adsorption,
23 elastic modulus and percolation probability, all of which are experimentally accessible.

24

25

26 Diffusion of small molecules, e.g. water, in porous media is of fundamental importance for
27 numerous applications including drug delivery, heterogeneous catalysis, adhesives, and many
28 others. Diffusion is usually characterized by the diffusion coefficient. Supplementary Note S1
29 clarifies the many definitions of diffusion coefficient, including intrinsic, tracer, corrected,
30 transport, mutual, self, chemical, and collective diffusion coefficients. Of note, this letter
31 focuses on self-diffusion, or equivalently, tracer diffusion [1]. Understanding how diffusion
32 coefficient is governed by the physical parameters of porous media has led to a plethora of
33 mechanistic models ranging from activation [2,3], hopping [4], obstruction [5], free volume [6–
34 8], to hydrodynamic/friction [9,10], etc.

35 For dilute polymer solutions, e.g. hydrogel (hydration typically higher than ~70%), diffusion
36 theories are relatively well established as fluid-solid interactions can be reasonably neglected
37 when pore size λ is much larger than the diffusant size σ , $\lambda \gg \sigma$. For example, the obstruction
38 theory successfully predicts diffusion coefficient in hydrogels by relating diffusion coefficient
39 to the probability of finding a pore large enough to accommodate water molecules [5]. In
40 contrast, for the case of highly concentrated polymer solutions, where $\lambda \sim \sigma$, the fluid-solid
41 interaction force ζ becomes dominant as it roughly scales with the reciprocal of the pore length
42 scale $\zeta \sim \lambda^{-1}$ (this is due to the fact that intermolecular solid/fluid forces are integrated over the
43 entire specific surface area which scales as the pore surface to volume ratio). This strong fluid-
44 solid interaction force leads to rich dynamics including molecular sieving, single-file diffusion,
45 anomalous diffusion, etc [10]. Tortuous pore structure superimposes additional complexity on
46 diffusion, whereas current diffusion theories have covered only simple pore geometries, such
47 as cylindrical and planar pores [11]. In short, the strong fluid-solid interaction and complex
48 pore structure form together a non-trivial energy landscape impeding the efforts of elucidating
49 diffusion when the size of the pore, also referred to as mesh opening or free volume,
50 approximates the water molecular size, $\lambda \sim \sigma$.

51 Besides the obstruction theory, researchers proposed free volume [6–8,12] and activation
52 energy-based theories [8,13]. Molecular studies have proved that free volume scales linearly
53 with adsorbed amount [12]. The experimental measurement of free volume remains
54 sophisticated, involving positron annihilation lifetime spectroscopy [14], inverse gas
55 chromatography [15], etc. [16], combined with semi-empirical interpretation. Though
56 activation energy can be more easily measured through temperature-dependent Arrhenius
57 processes [17,18], the connection between pore structure and activation energy, both relevant
58 to diffusion, is not straightforward. Moreover, the above mentioned theories do not consider
59 the intermittent dynamics of the diffusant. Previous works employed tortuosity, defined as the

60 ratio of self-diffusion coefficient of bulk water to water diffusion coefficient in pores $\xi = D_{s,w}$
61 $/D_{\mu}$, to phenomenologically describe the intermittent dynamics (however, we note that this
62 definition is not completely unambiguous as the in pore self-diffusivity can already differ from
63 the bulk due to confinement effects – i.e. even in the absence of residence times at the pore
64 surface). From a fundamental viewpoint, a microscopic explanation of tortuosity based on
65 physical parameters is still lacking.

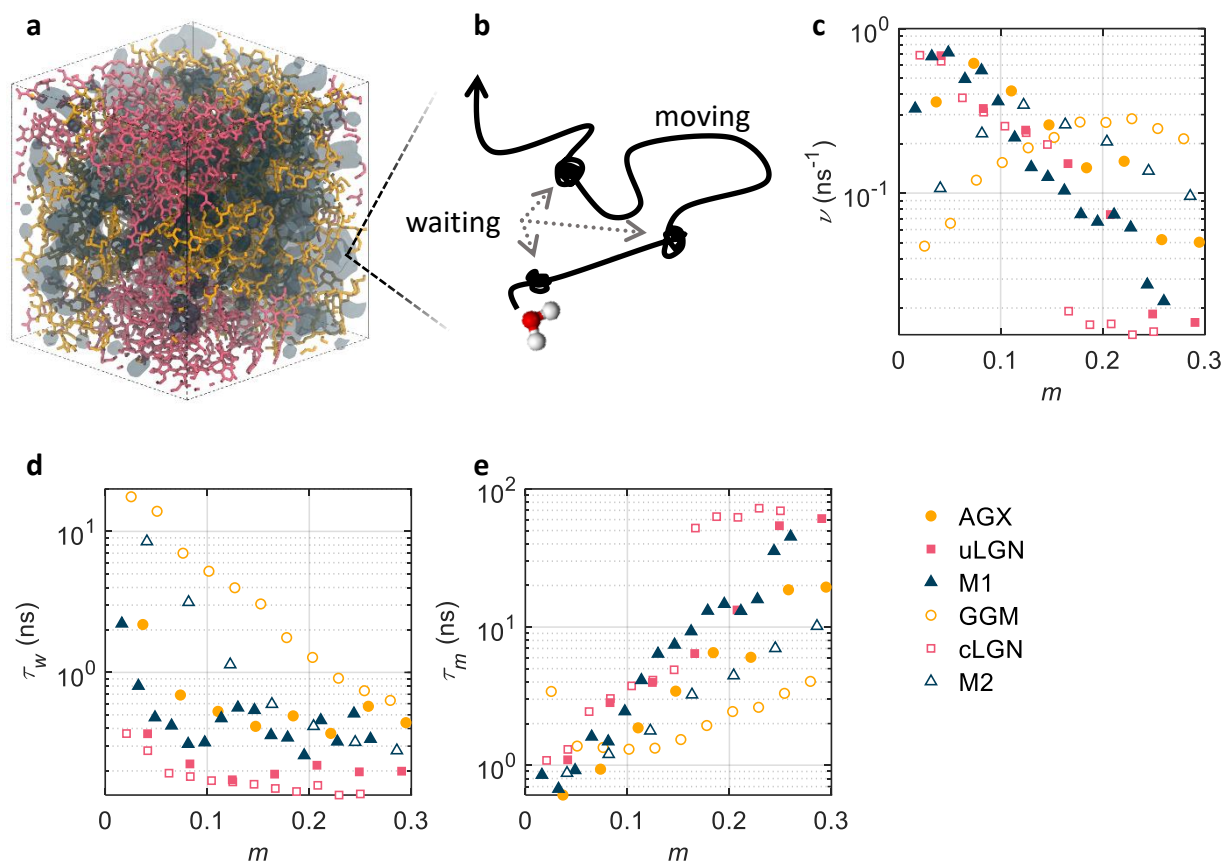
66 Continuum hypotheses break down at the subnanometer scale when $\lambda \sim \sigma$ [19]. In more detail,
67 from a thermodynamical point of view, confined water displays a complex behavior as the
68 interaction field generated by the host medium induces dynamical heterogeneities (e.g. [20]).
69 From a dynamical point of view, rich dynamic boundaries and non-viscous effects lead to
70 complex multiscale dynamics (e.g. [19,21]). To address water diffusion in a dense, sorptive and
71 deformable polymer structure, this study resorts to molecular dynamics (MD). We first
72 segregate microscopic diffusion coefficient from overall diffusion coefficient through the stop-
73 and-go formalism – which is equivalent to the concept of intermittent Brownian motion – and
74 then rationalize the concept of tortuosity using simple material parameters involving pore
75 structure, sorption and deformation. Our approach provides a unifying picture of the
76 intermittent motion of water molecules and of the quantification of complex diffusion landscape
77 through physically well-defined material parameters. This model provides a way of predicting
78 diffusion coefficients from adsorption heat, elastic modulus and percolation probability.

79 Six biopolymer systems are studied, i.e. two types of hemicelluloses, arabinoglucoronoxylan
80 (AGX) and galactoglucomannan (GGM), two types of lignins, uncondensed lignin (uLGN) and
81 condensed lignin (cLGN), and their mixtures, mixture 1 (M1, consisting of uLGN and AGX)
82 and mixture 2 (M2, consisting of cLGN and GGM). These polymer structures present in wood
83 are inspired and created following our previous work [22]. More details about the molecular
84 models are included in Supplementary Note S2. These wood polymers are chosen as model
85 systems because they cover a broad range of water-polymer interaction strengths, pore
86 structures, chain connectivities, etc. Moreover, water diffusion in wooden materials is relevant
87 to ubiquitous wooden building construction, furniture and artefacts, but also to more specialized
88 issues including archeological wood preservation [23], advanced wood-based iontronics
89 devices [24], etc. The moisture content, m , of the system is defined as the ratio of the mass of
90 water to the mass of the dry polymer. This study focuses on a moisture content range $m = 0-0.3$,
91 corresponding to the normal range of moisture load of wood exposed to humid
92 environments [25]. Figure 1a shows a sample mixture system M2 consisting of GGM and
93 cLGN at $m \sim 0.2$.

94 A typical simulation system has a lateral size of ~ 5 nm, containing $\sim 10,000$ atoms. The MD
95 simulations are carried out using GROMACS 5.0 package [26] and GROMOS 53a6 united-
96 atom force field [27] in isobaric-isothermal ensemble realized by velocity rescaling
97 thermostat [28] and Berendsen barostat [29]. The simulation time of each system is 100-1000
98 ns depending on the time needed to reach the Fickian diffusion regime, i.e. where the mean
99 square displacement (MSD) scales linearly with time. Sorption is mimicked by the random
100 insertion method (Supplementary Note S2) [22].

101 Diffusion is usually described using Einstein's equation where particle diffusion is considered
102 as random walk resulting from stochastic collisions. In sorptive systems, however, water
103 molecules move via a series of waiting – sometimes referred to as residence/stop/immobile –
104 and moving – relocation/go/mobile – events, alternatively identified as intermittent Brownian
105 dynamics [2–4,10,30,31]. We also observe such behavior and include a sample MSD curve in
106 Supplementary Note S3 (figure S1a) that displays alternating segments of plateaus and slopes,
107 corresponding to waiting and moving status, respectively. Figure 1b is the schematic of the
108 intermittent motion of a single water molecule.

109 Following our previous work [30], we define the time segment i , i.e. the time range $t_i < t < t_{i+1}$,
110 as waiting if the deviation from the average displacement is less than 0.1 nm (OH bond length),
111 $|\mathbf{r}(t) - \langle \mathbf{r} \rangle_t| < 0.1$ nm, $t \in [t_i, t_{i+1}]$, and the rate of change of its squared displacement
112 $\frac{d\mathbf{r}^2(t)}{dt} < 8 \times 10^{-8}$ nm² ns⁻¹, a value based on our visual observation of water trajectories. The
113 waiting time $\tau_w = t_{i+1} - t_i$ is then averaged over all waiting segments and water molecules. The
114 frequency of status switching, ν , is normalized by the total simulation time t_{tot} . Therefore, we
115 have $t_{\text{tot}} = t_w + t_m = \tau_w \nu t_{\text{tot}} + \tau_m \nu t_{\text{tot}}$, where $\nu^{-1} = \tau_w + \tau_m$ [33] and τ_m is the moving time.

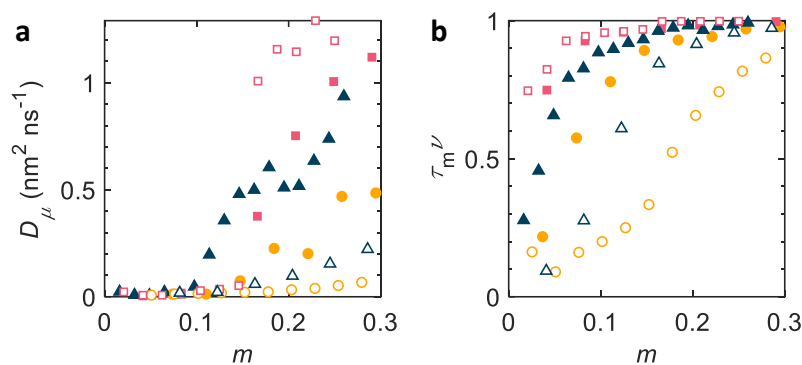


116

117 Figure 1 **a**) Sample system M2 at $m \sim 0.2$. The GGM, cLGN and water molecules are shown in
 118 yellow, pink and dark blue colors, respectively. **b**) Schematic of the intermittent motion of a
 119 single water molecule. **c**) Switching frequency ν . **d**) Waiting time τ_w . **e**) Moving time $\tau_m = \nu^{-1} -$
 120 τ_w .

121 The switching frequency ν is shown as a function of moisture content in Figure 1c for all
 122 systems. For the lignins uLGN and cLGN, the switching frequency monotonically decreases
 123 with moisture content. With ongoing hydration process, adsorption sites at polymer surface are
 124 gradually occupied by water molecules and, therefore, the new water molecules in the system
 125 are gradually screened from adsorption at the occupied sites and consequently remain mostly
 126 more mobile. For the same reason, with increasing moisture content m , the waiting time τ_w
 127 decreases while moving time τ_m increases as shown in Figure 1d and e. The switching frequency
 128 of the hemicellulose-containing systems displays a peak at intermediate moisture contents. This
 129 peak implies a crossover from waiting dominated mode to moving dominated mode, meaning
 130 that water molecules mostly stay waiting at low moisture content due to sorption, and are mostly
 131 moving at high moisture content [32]. Here, ergodicity is implicitly invoked, meaning that the
 132 fractions of moving and waiting molecules equal to the fraction of moving and waiting phases,
 133 respectively.

134 In the waiting state, water molecules are trapped, thus displaying a nearly zero diffusion
 135 coefficient. The real displacement only occurs during the moving phases (while this behavior
 136 is observed here, we note that in general surface diffusion in the adsorbed state can also be
 137 found). The diffusion coefficient in the moving phase is referred to as microscopic diffusion
 138 coefficient $D_\mu = D/(\tau_m \nu)$ [30]. The factor $\tau_m \nu$ denotes the fraction of moving water or time
 139 with respect to the total number of water or total time. The microscopic diffusion coefficient
 140 D_μ and the fraction of moving water molecules $\tau_m \nu$ are shown in Figure 2a and b.



141
 142 Figure 2 **a)** Microscopic diffusion coefficient. **b)** Fraction of moving water $\tau_m \nu$.

143
 144 The diffusion coefficient D is calculated as the slope of the Fickian regime averaged over all
 145 water molecules and time origins (Supplementary Note S1). For all systems, the diffusion
 146 coefficients increase with increasing moisture content but remain lower than the bulk water
 147 self-diffusion coefficient $D_{s,w} = 3.5 \text{ nm}^2 \text{ ns}^{-1}$ (the bulk diffusion coefficient was measured in a
 148 separate simulation). The cLGN and uLGN show the highest diffusion coefficient while GGM
 149 the lowest. M1 shows a diffusion coefficient lower than uLGN but higher than AGX, i.e. a
 150 mixing of its two components, and so is M2. We note that the diffusion coefficient of cLGN
 151 surges at $m \sim 0.15$. This is attributed to a special type of water molecule structure, i.e. the
 152 formation of percolation, defined as the emergence of a water cluster that penetrates through
 153 the whole system creating a continued diffusion channel which greatly enhances diffusion
 154 coefficient.

155 According to Figure 2b, the more hydrophilic hemicelluloses, i.e. AGX and GGM, show a
 156 lower fraction of moving status. Nonetheless, at high moisture content, all systems approach
 157 nearly full moving status, i.e. $\tau_m \nu \sim 1$. This means that few water molecules remain waiting at
 158 higher moisture content. It further implies that the microscopic diffusion coefficient is actually
 159 close to the diffusion coefficient, i.e. $D_\mu \sim D$. The more diffusive systems not only have a larger

160 fraction of moving status, but also the water inside those systems moves faster as suggested by
161 the higher D_μ .

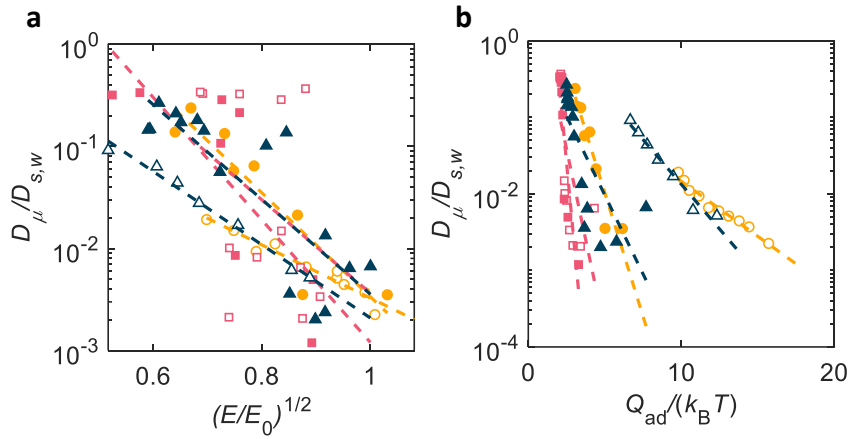
162 The mobility status is found to correlate with the polymer-water distance d_{pw} , defined as the
163 average distance between the oxygen atom of water and its nearest polymer atoms. The more
164 mobile water molecules locate further away from polymer, $d_{pw,m} > d_{pw,w}$, shown in figure S4.
165 Furthermore, d_{pw} can characterize the dispersity of water because it is related to the ratio of the
166 number of water at the surface of the cluster to the total number of water of the cluster, a
167 common measure of dispersity. Based on our results, water in hemicelluloses disperses better
168 than in lignins, a behavior which agrees with previous reports [22].

169 In the following, we analyse the behavior of the ratio $D_\mu/D_{s,w}$, which is the microscopic
170 diffusion coefficient D_μ normalized by the bulk self-diffusion coefficient, referred to as the
171 normalized diffusion coefficient. We note that the reciprocal of $D_\mu/D_{s,w}$ is often referred to as
172 tortuosity, $\xi = D_{s,w}/D_\mu$, interpreted as the degree of “detour” of the path taken by a diffusing
173 water molecule caused by the tortuous pore space. The normalized diffusion coefficient is
174 usually less than 1, $\xi^{-1} < 1$, because the diffusion coefficient in porous media is generally less
175 than the bulk self-diffusion coefficient of liquid water under the same thermodynamic
176 conditions.

177 Nanoporous biopolymer systems could represent sorptive, deformable and nanoporous
178 structures. This letter attempts to offer an alternative view of diffusion utilizing sorption and
179 deformability, which are quantitatively represented by adsorption heat Q_{ad} and elastic moduli
180 E , respectively. Measurement methods and results of these properties are described in
181 Supplementary Note S4 (figure S2). The normalized diffusion coefficient or tortuosity are
182 exponential functions of adsorption heat and elastic moduli, the justification of which is
183 discussed as follows.

184 In the activation theory, diffusion coefficient scales with the activation energy E_a , $D \sim \exp(-$
185 $E_a/k_B T)$. One can invoke a linear relationship between activation energy E_a of diffusion and heat
186 of adsorption, $E_a \sim \alpha Q_{ad}$ [33] (with α of the order but larger than 1 – in other words, the energy
187 barrier is larger than the energy difference between two states). Therefore, taking the limit $\alpha =$
188 1, an exponential relation between normalized diffusion coefficient can be employed, $\xi^{-1} \sim \exp(-$
189 $Q_{ad}/k_B T)$, where k_B and T denote Boltzmann constant and temperature, respectively. This
190 relation is shown to be valid, as seen in Figure 3b. It should be noted that in this study we take
191 liquid water as the reference state.

192 Yang and Chun derived the relation between diffusion coefficient and polymer persistence
 193 length $\ln D \sim l_p^{1/2}$ [34]. The persistence length of a worm-like chain is related to Young's
 194 modulus E , cross-section area, and moment of inertia M , following the relation $l_p = EM/k_B T$ [35].
 195 Therefore the normalized diffusion coefficient is also assumed to scale exponentially with
 196 Young's modulus, $\zeta^{-1} \sim \exp[(E/E_0)^{1/2}]$, where E_0 is for simplicity equal to 1 GPa only for making
 197 the term between brackets dimensionless. Figure 3c shows the validity of the proposed
 198 exponential scaling.



199
 200 Figure 3 Normalized diffusion coefficient in relation to **a)** heat of adsorption $Q_{ad}/k_B T$ and **b)**
 201 Young's modulus $(E/E_0)^{1/2}$ in a semi-log plot.

202 The prediction of diffusion coefficient based on heat of adsorption and elastic moduli works
 203 relatively well, as shown in Supplementary Note S5. However, for some systems, e.g. cLGN,
 204 there exists a surge of diffusion coefficient around $m \sim 0.15$, which is related to the occurrence
 205 of percolation. The prediction above, which relies on two terms (heat of adsorption and
 206 persistence length), fails to include such feature. It is thus necessary to introduce percolation
 207 into the model.

208 In this study, percolation is quantified by the percolation probability p_p defined as the time
 209 interval during which percolation is occurring divided by the total simulation time, i.e. $p_p =$
 210 $\int \delta_p(t) dt / \int dt$, where $\delta_p(t_i)$ equals 1 or 0 whether or not the system percolates at time t_i ,
 211 correspondingly (details in Supplementary Note S4). The scaling between normalized diffusion
 212 coefficient and percolation probability p_p is not a simple function. In analogy with heat of
 213 adsorption and modulus, we propose an exponential scaling, $\zeta^{-1} \sim \exp(p_p)$ (it will be shown
 214 afterwards that this mathematical form provides a reasonable description of the obtained results).
 215 In essence, percolation is a special type of structural feature that is not represented by heat of
 216 adsorption heat and elastic modulus, which support the inclusion of percolation as a separate

217 factor. The percolation probability is system size dependent. This study focuses on dense
 218 polymer networks with nanoscale pores which minimizes the impact of the size effect.

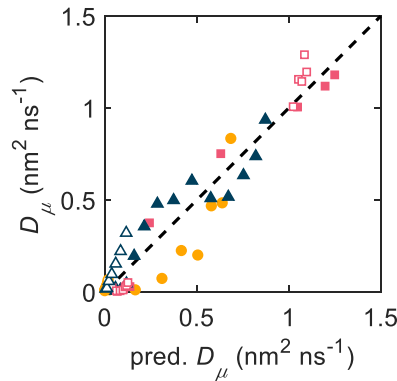
219 In spirit of tortuosity factorization [36], the abovementioned factors are multiplied in the
 220 sorption-deformation-percolation (SDP) model:

$$221 \quad \frac{1}{\exp(a_0)} \cdot \frac{D_\mu}{D_{s,w}} = \exp\left(a_Q \frac{Q_{ad}}{k_B T}\right) \cdot \exp\left(a_E \left(\frac{E}{E_0}\right)^{1/2}\right) \cdot \exp(a_p p_p)$$

222 where a_i ($i = 0, Q, E$ or p) is weight. We can also write

$$\ln \frac{D_\mu}{D_{s,w}} = a_0 + a_Q \frac{Q_{ad}}{k_B T} + a_E \left(\frac{E}{E_0}\right)^{1/2} + a_p p_p$$

223 The SDP model well describes the measurements as shown in Figure 4. A sensitivity analysis
 224 is carried out by omitting an arbitrary number of factors. The prediction power is poor for any
 225 model with fewer factors.



226
 227 Figure 4 Measured and predicted diffusion coefficient D_μ .

228 The weights are $a_0 = -0.572$, $a_Q = -3.051$, $a_E = -1.243$ and $a_p = 0.466$. The weights a_i in the SDP
 229 model are dimensionless numbers, which are the first derivative of $\ln \zeta^{-1}$ with respect to the
 230 corresponding property x_i , $a_i = \partial \ln \zeta^{-1} / \partial x_i$. The a_0 is introduced to manifest all the influencing
 231 factors other than sorption, deformation and percolation. Especially, when a_Q is zero, the SDP
 232 model reduces to the description of non-sorptive material. Previous diffusion models generally
 233 focus on systems where host-guest interaction is negligible and the pore length scale is much
 234 larger than the diffusant size. Here we show that the SDP model well describes dense, sorptive
 235 and deformable polymer materials, e.g. nanoporous biopolymers.

236 The model can potentially be verified by experiments. Diffusion coefficient D can be measured
 237 via nuclear magnetic resonance (NMR). The waiting and moving statistics are accessible via
 238 experimental methods such as differential scanning calorimetry (DSC) and NMR [37]. In fact,

239 our simulation shows that water in most systems is mainly in the moving state, except for the
240 strongly adsorbing material, GGM, whose heat of adsorption reaches $\sim 43 \text{ kJ mol}^{-1}$. It is noted
241 that the latent heat of water is not included as we use liquid water as the reference state (details
242 in Supplementary Note S4). The proposed material parameters of tortuosity are also
243 experimentally accessible: heat of adsorption Q_{ad} and Young's modulus E can be measured via
244 calorimetry and mechanical tests, respectively; the probability of percolation can be estimated
245 by e.g. conductivity or capacitance. Preliminary validation of the SDP model based on literature
246 data is included in Supplementary Note S7 where acceptable agreement between the predicted
247 and measured diffusion coefficient is shown.

248 While this study focuses on water diffusion, we believe that our framework can be extended to
249 other diffusants, such as hydrated ions, methane, etc., as long as the molecular size
250 approximates the size of the free volume or pore length scale. For instance, most drugs have
251 molecular sizes around 0.5-5 nm which are comparable to the pore length scale of the drug
252 delivery systems. Better control of drug release can be achieved by the rational design of the
253 structure of the host porous media under the guidance of our model.

254 The polymer-water distance d_{pw} is found to be strongly correlated with heat of adsorption Q_{ad} ,
255 as shown in figure S4. This offers an alternative way of characterizing sorption. Replacing Q_{ad}
256 with d_{pw} in SDP model give equivalently good results, which further demonstrates that they
257 carry the same information and can thus be used interchangeably.

258 To sum up, this study offers a unifying picture of water diffusion within dense disordered
259 porous media, and moreover describes diffusion coefficient via a complete set of physically
260 well-defined material properties. We resort to MD simulations where the trajectories of
261 individual water molecules manifest the intermittent dynamics which is caused by strong
262 sorption interactions and highly tortuous pore space. The microscopic diffusion coefficient D_{μ}
263 should be extracted from the measured diffusion coefficient D by disregarding the waiting
264 phases using factor τ_{mv} , the fraction of moving water derived from single water molecule
265 statistics. The microscopic diffusion coefficient, equivalently tortuosity ζ , is then predicted via
266 three characteristic parameters of the porous media, i.e. heat of adsorption Q_{ad} , Young's
267 modulus E and probability of percolation p_p , each representing a fundamental physical aspect
268 of the porous system, i.e. sorption, deformation and percolating structure. The SDP model,
269 therefore, provides guidelines for the comparison of diffusion in different polymers. The model
270 may guide the design of materials to achieve desired diffusion property.

271

272
273
274
275
276
277
278
279
280
281
282
283
284
285
286
287
288
289
290
291
292
293
294
295
296
297
298
299
300
301

Supplementary material:

Funding: The authors acknowledge the support of the Swiss National Science Foundation (SNSF) [grant No. 162957].

References

- [1] J. Kärger and D. M. Ruthven, *Diffusion in Nanoporous Materials: Fundamental Principles, Insights and Challenges*, New J. Chem. **40**, 4027 (2016).
- [2] A. T. DiBenedetto and D. R. Paul, *An Interpretation of Gaseous Diffusion through Polymers Using Fluctuation Theory*, J. Polym. Sci. Part A Gen. Pap. **2**, 1001 (1964).
- [3] P. Meares, *The Diffusion of Gases Through Polyvinyl Acetate I*, J. Am. Chem. Soc. **76**, 3415 (1954).
- [4] F. M. Preda, A. Alegría, A. Bocahut, L. A. Fillot, D. R. Long, and P. Sotta, *Investigation of Water Diffusion Mechanisms in Relation to Polymer Relaxations in Polyamides*, Macromolecules **48**, 5730 (2015).
- [5] N. A. Hadjiev and B. G. Amsden, *An Assessment of the Ability of the Obstruction-Scaling Model to Estimate Solute Diffusion Coefficients in Hydrogels*, J. Control. Release **199**, 10 (2015).
- [6] J. S. Vrentas and J. L. Duda, *Diffusion in Polymer—Solvent Systems. I. Reexamination of the Free-Volume Theory*, J. Polym. Sci. Polym. Phys. Ed. **15**, 403 (1977).
- [7] H. Fujita, *Diffusion in Polymer-Diluent Systems*, in *Fortschritte Der Hochpolymeren-Forschung* (Springer-Verlag, Berlin/Heidelberg, 1961), pp. 1–47.
- [8] K. Falk, B. Coasne, R. Pellenq, F. J. Ulm, and L. Bocquet, *Subcontinuum Mass Transport of Condensed Hydrocarbons in Nanoporous Media*, Nat. Commun. **6**, 6949 (2015).
- [9] R. I. Cukier, *Diffusion of Brownian Spheres in Semidilute Polymer Solutions*, Macromolecules **17**, 252 (1984).
- [10] C. Bousige, P. Levitz, and B. Coasne, *Bridging Scales in Disordered Porous Media by Mapping Molecular Dynamics onto Intermittent Brownian Motion*, Nat. Commun. **12**, 1 (2021).

- 302 [11] B. Coasne, *Multiscale Adsorption and Transport in Hierarchical Porous Materials*,
303 New J. Chem. **40**, 4078 (2016).
- 304 [12] A. Obliger, R. Pellenq, F.-J. Ulm, and B. Coasne, *Free Volume Theory of Hydrocarbon*
305 *Mixture Transport in Nanoporous Materials*, J. Phys. Chem. Lett. **7**, 3712 (2016).
- 306 [13] R. M. Barrer, *The Zone of Activation in Rate Processes*, Trans. Faraday Soc. **39**, 237
307 (1943).
- 308 [14] G. Dlubek, A. P. Clarke, H. M. Fretwell, S. B. Dugdale, and M. A. Alam, *Positron*
309 *Lifetime Studies of Free Volume Hole Size Distribution in Glassy Polycarbonate and*
310 *Polystyrene*, Phys. Status Solidi Appl. Res. **157**, 351 (1996).
- 311 [15] Y. P. Yampolskii, N. E. Kaliuzhnyi, and S. G. Durgarjan, *Thermodynamics of Sorption*
312 *in Glassy Poly(Vinyltrimethylsilane)*, Macromolecules **19**, 846 (1986).
- 313 [16] J. C. Jansen, M. MacChione, E. Tocci, L. De Lorenzo, Y. P. Yampolskii, O. Sanfirova,
314 V. P. Shantarovich, D. Hofmann, and E. Drioli, *Comparative Study of Different*
315 *Probing Techniques for the Analysis of the Free Volume Distribution in Amorphous*
316 *Glassy Perfluoropolymers*, Macromolecules **42**, 7589 (2009).
- 317 [17] W. W. Brandt, *Model Calculation of the Temperature Dependence of Small Molecule*
318 *Diffusion in High Polymers*, J. Phys. Chem. **63**, 1080 (1959).
- 319 [18] A. T. DiBenedetto, *Molecular Properties of Amorphous High Polymers. II. An*
320 *Interpretation of Gaseous Diffusion through Polymers*, J. Polym. Sci. Part A Gen. Pap.
321 **1**, 3477 (1963).
- 322 [19] L. Bocquet and E. Charlaix, *Nanofluidics, from Bulk to Interfaces*, Chem. Soc. Rev. **39**,
323 1073 (2010).
- 324 [20] B. Coasne, A. Galarneau, F. Di Renzo, and R. J. M. Pellenq, *Molecular Simulation of*
325 *Adsorption and Intrusion in Nanopores*, Adsorption **14**, 215 (2008).
- 326 [21] C. Cottin-Bizonne, J. L. Barrat, L. Bocquet, and E. Charlaix, *Low-Friction Flows of*
327 *Liquid at Nanopatterned Interfaces*, Nat. Mater. **2**, 237 (2003).
- 328 [22] C. Zhang, M. Chen, S. Keten, B. Coasne, D. Derome, and J. Carmeliet,
329 *Hygromechanical Mechanisms of Wood Cell Wall Revealed by Molecular Modeling*
330 *and Mixture Rule Analysis*, Sci. Adv. **7**, (2021).
- 331 [23] E. Hocker, G. Almkvist, and M. Sahlstedt, *The Vasa Experience with Polyethylene*
332 *Glycol: A Conservator's Perspective*, J. Cult. Herit. **13**, S175 (2012).

- 333 [24] T. Li et al., *A Nanofluidic Ion Regulation Membrane with Aligned Cellulose*
334 *Nanofibers*, *Sci. Adv.* **5**, eaau4238 (2019).
- 335 [25] A. J. Stamm, *Wood and Cellulose Science* (Ronald, 1964).
- 336 [26] M. J. Abraham, T. Murtola, R. Schulz, S. Páll, J. C. Smith, B. Hess, and E. Lindah,
337 *Gromacs: High Performance Molecular Simulations through Multi-Level Parallelism*
338 *from Laptops to Supercomputers*, *SoftwareX* **1–2**, 19 (2015).
- 339 [27] C. Oostenbrink, A. Villa, A. E. Mark, and W. F. Van Gunsteren, *A Biomolecular Force*
340 *Field Based on the Free Enthalpy of Hydration and Solvation: The GROMOS Force-*
341 *Field Parameter Sets 53A5 and 53A6*, *J. Comput. Chem.* **25**, 1656 (2004).
- 342 [28] G. Bussi, D. Donadio, and M. Parrinello, *Canonical Sampling through Velocity*
343 *Rescaling*, *J. Chem. Phys.* **126**, 014101 (2007).
- 344 [29] H. J. C. Berendsen, J. P. M. Postma, W. F. van Gunsteren, A. DiNola, J. R. Haak, J. P.
345 M. van Postma, W. F. van Gunsteren, A. DiNola, and J. R. Haak, *Molecular Dynamics*
346 *with Coupling to an External Bath*, *J. Chem. Phys.* **81**, 3684 (1984).
- 347 [30] K. Kulasinski, R. Guyer, D. Derome, and J. Carmeliet, *Water Diffusion in Amorphous*
348 *Hydrophilic Systems: A Stop and Go Process*, *Langmuir* **31**, 10843 (2015).
- 349 [31] A. Malani and K. G. Ayappa, *Relaxation and Jump Dynamics of Water at the Mica*
350 *Interface*, *J. Chem. Phys.* **136**, 194701 (2012).
- 351 [32] C. Zhang, B. Coasne, R. Guyer, D. Derome, and J. Carmeliet, *Moisture-Induced*
352 *Crossover in the Thermodynamic and Mechanical Response of Hydrophilic*
353 *Biopolymer*, *Cellulose* **27**, 89 (2020).
- 354 [33] V. J. Inglezakis and A. A. Zorpas, *Heat of Adsorption, Adsorption Energy and*
355 *Activation Energy in Adsorption and Ion Exchange Systems*, *Desalin. Water Treat.* **39**,
356 149 (2012).
- 357 [34] Y. Yang and M.-S. Chun, *The Effect of Chain Stiffness on Moisture Diffusion in*
358 *Polymer Hydrogel by Applying Obstruction-Scaling Model*, *Korea-Australia Rheol. J.*
359 **25**, 267 (2013).
- 360 [35] C. G. Baumann, S. B. Smith, V. A. Bloomfield, and C. Bustamante, *Ionic Effects on*
361 *the Elasticity of Single DNA Molecules*, *Proc. Natl. Acad. Sci.* **94**, 6185 (1997).
- 362 [36] A. Boğan, F.-J. Ulm, R. J.-M. Pellenq, and B. Coasne, *Bottom-up Model of Adsorption*
363 *and Transport in Multiscale Porous Media*, *Phys. Rev. E* **91**, 032133 (2015).

364 [37] T. Hatakeyama, M. Tanaka, A. Kishi, and H. Hatakeyama, *Comparison of*
365 *Measurement Techniques for the Identification of Bound Water Restrained by*
366 *Polymers*, *Thermochim. Acta* **532**, 159 (2012).

367

368

369